INTERNATIONAL SOCIETY FOR SOIL MECHANICS AND GEOTECHNICAL ENGINEERING



This paper was downloaded from the Online Library of the International Society for Soil Mechanics and Geotechnical Engineering (ISSMGE). The library is available here:

https://www.issmge.org/publications/online-library

This is an open-access database that archives thousands of papers published under the Auspices of the ISSMGE and maintained by the Innovation and Development Committee of ISSMGE.

The paper was published in the proceedings of the 20th International Conference on Soil Mechanics and Geotechnical Engineering and was edited by Mizanur Rahman and Mark Jaksa. The conference was held from May 1st to May 5th 2022 in Sydney, Australia.

A scalable three-dimensional multiscale framework for modeling of granular column collapse

Un cadre multi-échelle tridimensionnel évolutif pour la modélisation de l'effondrement de colonnes granulaires

Weijian Liang & Jidong Zhao

Department of Civil and Environmental Engineering, Hong Kong University of Science and Technology, Kowloon, Hong Kong, wliangab@connect.ust.hk

ABSTRACT: This study presents a scalable three-dimensional (3D) multiscale framework to model large deformation of granular media. The multiscale framework features a hierarchical coupling of a continuum approach Material Point Method (MPM) and a discrete approach Discrete Element Method (DEM) for cross-scale simulation of boundary value problems. Specifically, the MPM is used to solve the governing equations of a macroscopic boundary value problem that may enter the large deformation regime, while the DEM is used to provide the path-dependent mechanical response required at each material point of MPM based on grain-scale, contact-based simulations. The innovative bridging of MPM and DEM allows to easily tackle large deformation problems in geomechanics while bypassing the requirement of a presumed constitutive model typically exceedingly complicated in continuum approach. To mitigate the pertinent computation cost for 3D large-scale simulations, we further propose an effective, scalable Message Passing Interface (MPI) based parallel scheme for the multiscale approach and port it onto the Tianhe 2 supercomputer. Simulations of the collapse of a three-dimensional granular column are conducted and results on the rheology of the collapsing column and the evolution of macroscopic energy are examined and discussed. The study demonstrates the predictive power of multiscale modeling in solving practical problems of granular media.

KEYWORDS: multiscale modeling; three-dimension; Message Passing Interface (MPI); column collapse

1 INTRODUCTION.

Granular materials are ubiquitous in our daily life. However, it is still challenging to accurately predict the mechanical responses of granular materials in a setting of engineering-scale applications due to the underlying grains interaction. Recently, hierarchical multiscale modeling has been flourishing in computational geomechanics, in an attempt to provide the community a next-generation numerical analysis toolbox for tackling these obstacles. These multiscale frameworks mainly deploy Discrete Element Method (DEM) to provide micromechanics-based solutions for upscaled continuum approaches, like FEM (Guo & Zhao, 2014), MPM (Liang & Zhao, 2019) or Smooth Particle Finite Element Method (SPFEM) (Guo et al., 2021), bypassing the use of phenomenological constitutive laws. These approaches have showcased promising capacity in typical engineering applications, like borehole instability (Wu et al. 2018) and pullout of anchor (Liang et al. 2021).

Due to the excessive computational intensity, most multiscale modeling applications so far are constrained in two-dimensional (2D) scenarios. Although 2D multiscale modeling based on plane strain/stress assumptions can offer unique insights into certain problems, it is not without limitations. The first one is related to the DEM solver by which the mechanical behavior of granular materials is reproduced. Using discs (2D) to represent granular grains, all out-of-plane grain motions and inter-particle interactions are prohibited. Despite such constraints can render a qualitatively sound behavior of the granular media, the predictions may not be quantitatively comparable with experimental data (e.g., porosity, peak/residual stress, and dilatancy). Meanwhile, it is well-known that macroscopic phenomena of granular materials are controlled not only by the mechanical properties of specimens but also by the geometry setting and the loading conditions. A representative example is the compression test on a sandy soil specimen. For a denselypacked sample, cross-shape shear bands are commonly observed under plane strain setting, whereas octopus-shaped shear localization zone and diffuse failure may occur under triaxial compression or extension (Guo and Zhao 2016). Moreover, the

2D setting may also prohibit modeling of some practical problems, such as debris flow which naturally occurs in mountainous areas with complex terrain. Given these issues, it is of great importance to implement a fully 3D multiscale framework and facilitate more accurate and realistic modeling of practical engineering problems.

Although the extension from 2D to 3D is conceptually straightforward, it remains challenging from an implementation perspective. A crucial issue needed to be addressed for 3D multiscale modeling is how to handle the arising tremendous computational cost. Typically, for a 3D MPM simulation, the number of material points involved is at least one order larger than that in 2D. Moreover, the Representative Element Volume (RVE) that is used to obtain mechanical responses of media also has to contain more grain particles. These two factors jointly render 3D multiscale modeling to be more computationally expensive compared to its 2D counterpart and therefore demanding a high-performance solution.

In this study, an efficient and scalable parallel scheme is proposed for the hierarchical multiscale framework, taking the advantage of flagship supercomputing facilities, to solve 3D large-scale problems. In what follows, the multiscale framework is briefed and the proposed parallel scheme is elaborated. Then its performance will be also evaluated by the simulation of the 3D granular column collapse. Finally, results on the rheology of the collapsing column and the evolution of macroscopic energy will be discussed.

2 MULTISCALE FRAMEWORK AND PARALLELISM

The multiscale framework in this study is established through a hierarchical coupling of a continuum approach MPM and a discrete approach DEM. Specifically, the MPM is used to solve

kinematics and deformation of a continuum which is governed by the following equations of conservation:

$$\frac{\mathbf{D}\rho}{\mathbf{D}t} = 0$$

$$\rho \frac{\mathbf{D}v}{\mathbf{D}t} = \nabla \cdot \boldsymbol{\sigma} + \rho g$$
(1)

$$\rho \frac{\mathbf{D}v}{\mathbf{P}t} = \nabla \cdot \boldsymbol{\sigma} + \rho g \tag{2}$$

where ρ is density; \boldsymbol{v} denotes velocity; $\boldsymbol{\sigma}$ is Cauchy stress and g is the gravity acceleration. Since the mass of individual material points in MPM remains unchanged throughout the simulation, the mass conservation (Eqn. 1) is automatically satisfied. While the momentum equation could be solved accordingly on the background mesh in a similar manner as FEM. For conventional MPM, a constitutive model describing the strain-stress relation is required to close the system. However, within the MPM-DEM multiscale framework, the nonlinear, path-dependent mechanical responses of granular media are provided by DEM through grain-scale, contact-based simulations on RVE. For a DEM assembly, the Cauchy stress σ is computed based on the Love-Weber formula (Christoffersen et al, 1981; Nicot et al, 2013) which reads:

$$\sigma = \frac{1}{V_{RVF}} \sum_{N_c} \mathbf{d} \otimes \mathbf{f}^c \tag{3}$$

where V_{RVE} is the volume of the RVE; N_c is the amount of contact within the packing; d represents the branch vector joining centroids of two particles in contact and f^c denotes the contact force. The innovative bridging of MPM and DEM allows to easily tackle large deformation problems in geotechnical engineering while bypassing presumed phenomenological constitutive models.

In the present multiscale framework, two codes, CB-Geo MPM and YADE are deployed for MPM and DEM solver, respectively. Since shearing RVE in DEM is the most computationally expensive part of the entire computation, the large-scale parallelism across distributed compute nodes is merely implemented for accelerating the DEM computation, while the MPM which is less expensive is only handled among different threads within a single node using Intel Threading Building Blocks (TBB) for simplicity.

The proposed parallel is favorable for massively parallel CPU cores within a torus network. Central to the proposed parallel scheme is the data and task parallelism. The parallel scheme implementation is based on a single-level flat MPI model and could be graphically illustrated in Fig. 1. Prior to the explicit time integration, the set containing the entire material points index is divided nearly evenly into $\mathcal N$ partitions ($\mathcal N$ is equal to the number of MPI processes) and distributed to all MPI processes. With assigned indexes, the DEM solver in each process could load corresponding RVE packings into local memory. Loading packing into separated processing units helps to achieve data parallelism, minimizing data exchange between the master and slave threads and hence reducing the communication overhead. Operations in subsequent coupling cycles are executed in a similar manner. Firstly, the incremental deformation gradients for all RVEs are computed in the MPM solver. Then they are distributed to all MPI threads by a collective communication routine MPI_SCATTER. Based on these deformation information, the task of shearing RVE, which is the most computationally intensive part within the entire workflow, is undertaken by all MPI processes concurrently. Once the task of shearing RVE is finished across all processing units, material responses (i.e., Cauchy stress and averaged particle rotation) will be retrieved from the deformed RVE and sent back to the master rank (via MPI GATHER) for subsequent computations in the MPM solver, such as updating the motions and positions of material points.

This 3D multiscale framework is further installed onto Tianhe-2 at the Guangzhou National Supercomputer Centre to give a full play to the proposed parallel scheme. As a top-ranking supercomputer, Tianhe-2 has around 16 000 nodes with each equipped with 2-way 12-core Intel Xeon E5-2692v2 CPU, 3x Intel Xeon Phi coprocessor, 64GB memory and customized internal high-speed interconnection TH-2 Express-2. It is noted that although the proposed framework is run on massively largescale architectures such as Tianhe-2, it is also suitable for medium-size clusters as well as common desktops since it is developed for the standard Linux environment despite the problems size may be constrained due to the memory limitation

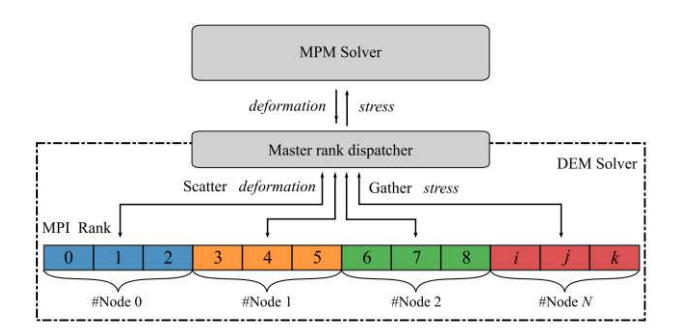


Figure 1. Illustration of the parallel scheme for MPM-DEM multiscale

MODELING 3D GRANULAR COLUMN COLLAPSE

In this section, a 3D granular column collapse is modeled to evaluate the performance of the proposed parallel scheme as well as to demonstrate the potential of the 3D multiscale approach.

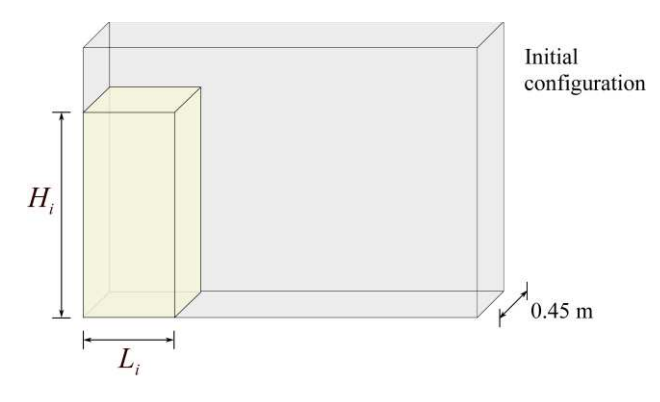
3.1 Model setup

The model setup for the simulation is shown in Fig. 2. The slumping is carried out within a rectangular chamber with a width of 0.45m. The dimensions of the granular column are denoted by L(length) and H(height). The subscript "i" and "f" represent the initial and final state, respectively. In the current study, H_i is set to 1.32m, L_i is set to 0.55m and the aspect ratio for the column $a = H_i/L_i$ is equal to 2.4. The whole simulation domain is discretized by hexahedron elements with an element size of 0.05m. It is worth pointing out that the dimension selected for the simulation has been scaled up 10 times compared to the experimental setting (Lajeunesse et al. 2005) for a larger time step size. The bed of the chamber is assumed to be rough while the side walls are set to be frictionless. Before the commencement of the collapse, RVE packings to be embedded to material points are prepared based on the microscopic parameters listed in Table 1.

The entire simulation is divided into two stages: in the first stage, an additional Dirichlet boundary condition (velocity constraint) is imposed at the lateral free surface of the column to achieve a stable, equilibrium state. While in the second one, this constraint is removed, and the column could flow down freely.

Table 1. Microscopic parameters in DEM solver

Parameter	Symbol[unit]	Value
Number of particles	N_p	800
Radius	r[mm]	0.92-1.38
density	$\rho[{ m kg/m^3}]$	2500
Young's modulus	E[MPa]	600
Interparticle friction	μ	0.518



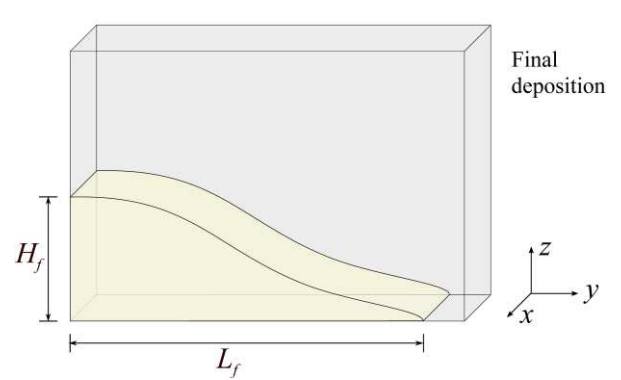


Figure 2. Model setup for 3D granular column collapse

3.2 Parallel performance

In the current simulation, the granular column contains 65 882 RVEs. With each comprising 800 DEM particles, the problem size involves up to 52,705,600 grains. The simulation is carried out on Tianhe-2 supercomputer hosted in Guangzhou, China and the elapsed wall clock time is around 10 hours with 16 nodes (384 CPU cores).

To measure the performance of the parallel scheme, we carry out a strong scaling test (fixed workload) for the same problem. In the scaling test, the computation runs 500 steps with 1 to 256 compute nodes (CPU cores ranges from 24 to 6144), and the corresponding elapsed time is recorded as $t_{N_{node}}$. Given the computation time, it is straightforward to obtain the parallel acceleration by the speedup factor: $speedup = t_1/t_{N_{node}}$. In addition, the execution time for the MPM part, DEM part, and MPI communication in each coupling cycle are also recorded for analysis. Particularly, the cost of MPM includes computing deformation gradient for all RVEs and updating motions and positions of material points, the cost of MPI includes scattering the deformation information and gathering homogenized stresses while the DEM cost refers to the time needed to load all RVEs with prescribed boundary conditions. Since the output step

(generate .vtk file) is only executed every thousand steps in typical practice, it is not included in this scaling test.

The execution time profile in the strong scaling test is shown in Fig. 3. As indicated by the case with $N_{node} = 1$, the DEM simulation in each step takes around 17.9 s, constituting up about 97.7% of the overall elapsed time. This proportion is so high that it is reasonable to pay efforts to improve this specified part as done by this study. With more nodes utilized, the cost of DEM drops substantially, which appears to be inversely proportional to the number of nodes. While for the MPM part, the computational cost remains around 0.36 s since no MPI-based parallel scheme is implemented for MPM computation.

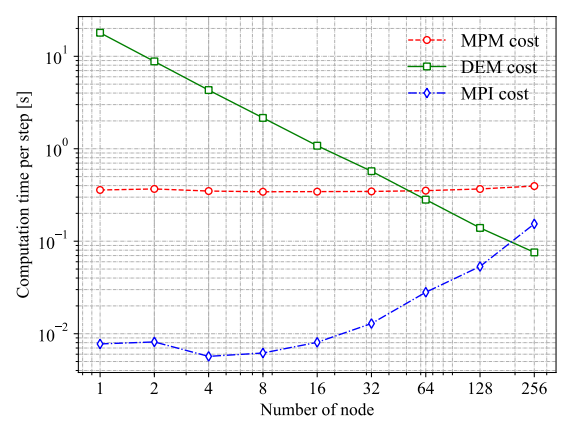


Figure 3. Averaged execution time per step for each part of the computation in strong scaling test

Fig. 4 shows the parallel acceleration against the number of nodes. For comparison purposes, we also include the ideal scaling and the prediction by Amdahl's Law in the figure. Amdahl's Law states that the upper limit of the speedup can be achieved in a strong scale test can be described by following

$$speedup = 1/(s + \frac{p}{N_{node}}) \tag{4}$$

where *s* and *p* are the fractions of serial and parallel parts within the entire computation. As shown in Fig. 4, the multiscale modeling could be significantly accelerated by the proposed efficient and scalable parallel scheme. Specifically, the proposed parallel scheme can achieve an ideal linear parallel acceleration for the DEM part across all cases tested. While for the overall computation, the speedup is up to 26.77 for 64 nodes and 31.66 for 128 nodes, which agrees well with Amdahl's Law prediction. It is also observed that there is a minor drop in the speedup when using 256 nodes. This performance loss is mainly due to the increase in communication overhead exceeds the reduction in DEM computation as depicted in Fig. 3.

3.3 Flow rheology and energy evolution

For the granular column collapse, its flow rheology is first studied. Fig. 5 shows snapshots of the velocity field of the column during the collapse. A dimensionless characteristic time t^* is used in the analysis, which is related to the free fall of the granular column via the following equation:

$$t^* = \sqrt{H_i/g} \tag{5}$$

where g is the gravity. The characteristic time is computed as $t^* = 0.367$ s in the current setting. From Fig. 5, it is observed that the failure is initiated from the bottom of the outer surface of the

column. In the early stage, the slip surface is around 45° to the ground surface. This failure surface keeps propagating and tilling slightly upwards. For the mobilized mass, its upper part tends to fall freely while the lower part slice along the failure plane. At $t = 3t^*$, the majority of the column ceases moving and only those close to the toe move slowly. At $t = 6t^*$, the whole column deposits completely and the final deposition is in a wedge shape. It is also observed the runout distance of this study is slightly smaller than the experimental result (Lajeunesse et al. 2005). The underestimation of the runout distance is because the simulation adopts a relatively large element size (0.05 m) and the displacement constraint in the base to be more noticeable.

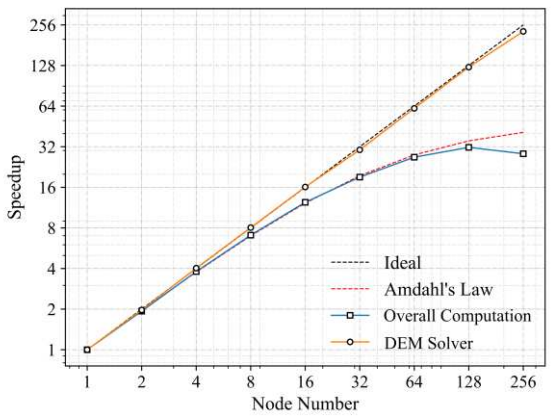


Figure 4. Computation speedup versus node number in strong scaling test

The collapse process is commonly accompanied by apparent particle rotations. Herein, we extract the average particle rotation θ from RVEs for analysis which is defined as:

$$\overline{\boldsymbol{\theta}} = \frac{1}{N_p} \sum_{N_p}$$
 (6)

where N_p is the number of particles within the packing and . Fig. 6 shows the average particle rotation for the granular column at the final state. It appears that the soil close to the corner of the chamber does not experience any particle rotation, manifesting itself as a static zone throughout the collapse process. As such, the average particle rotation may serve as an alternative indicator to defines the interface between the static zone and flow layer which is somehow blurred to define by merely velocity field because of the continuous development during the whole process.

Finally, the evolution of energy is also investigated. The potential energy E_p , kinetic energy E_k and dissipated energy E_d can be computed as follow:

$$E_{p} = \sum_{i=1}^{N_{mp}} m_{i}gz_{i}$$
 (7)

$$E_{k} = \sum_{i=1}^{N_{mp}} \frac{1}{2}m_{i}v_{i}^{2}$$
 (8)

$$E_{d} = E_{p}^{0} - E_{p} - E_{k}$$
 (9)

$$E_k = \sum_{i=1}^{N_{mp}} \frac{1}{2} m_i v_i^2 \tag{8}$$

$$E_d = E_n^0 - E_n - E_{\nu} \tag{9}$$

where E_p^0 is the initial potential energy, N_{mp} is the number of material points, m, z, and v are the mass, the height, and the translational velocity of an individual material point. Fig. 7 depicts the evolution of normalized energy. During a short period immediately after the collapse, the potential energy decrease and partially converts to kinetic energy. After the collapse process is fully developed, the kinetic energy starts to decrease steadily while the dissipated energy raises rapidly until a constant value is reached $E_d/E_p^0 = 0.549$.

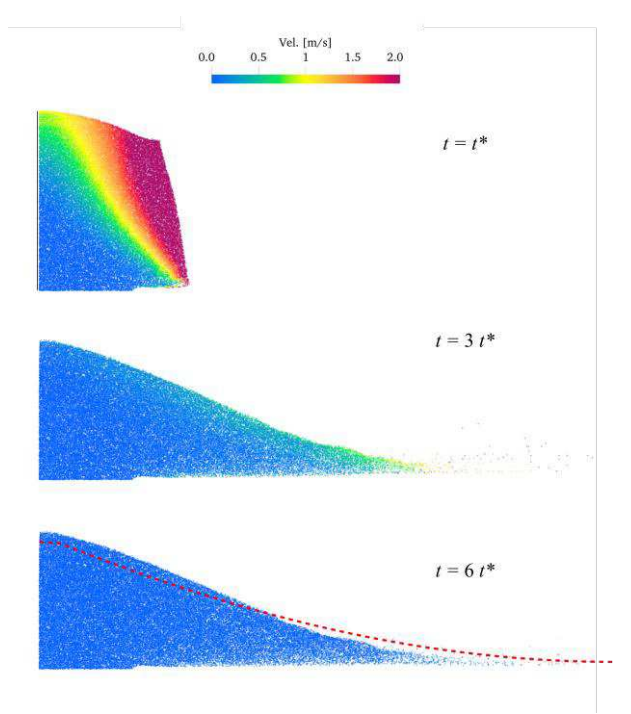


Figure 5. Snapshots of the velocity field for the granular column in t = t^* , $3t^*$ and $6t^*$. The dashed line in $t = 6t^*$ indicates the scaled soil configuration in experimental test (Lajeunesse et al. 2005)

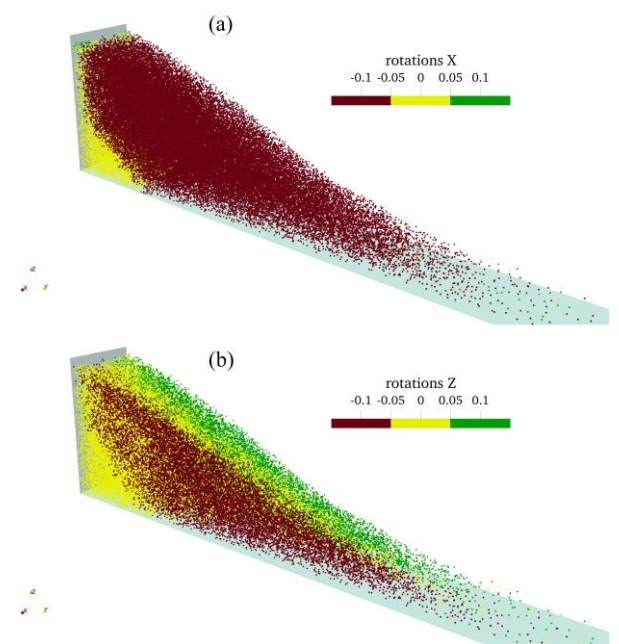


Figure 6. Accumulated averaged particle rotation at the final state

instabilities in high-porosity sandstones. *Journal of Geophysical Research: Solid Earth*, 123(5), 3450-3473.

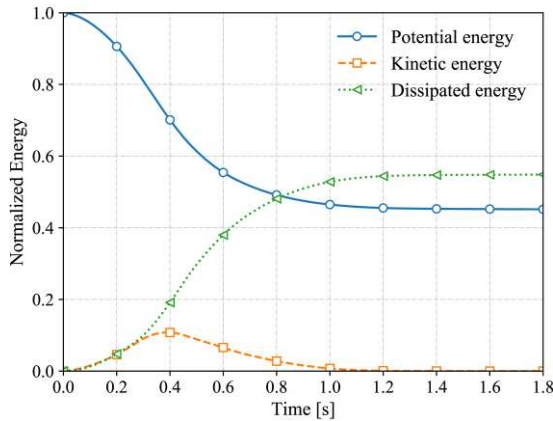


Figure 7. Evolution of normalized potential, kinetic, and dissipated energy

4 CONCLUSIONS

This study presents a three-dimensional multiscale framework for modeling large-scale problems of granular materials. To mitigate the pertinent computation cost for 3D large-scale simulations, we propose an effective and scalable MPI-based parallel scheme for the multiscale approach and further implemented it onto flagship supercomputing facilities. This proposed parallel scheme could achieve a computation acceleration of 31.66 using 128 nodes on the Tianhe-2 supercomputer. The predictive power of the multiscale approach equipped is also demonstrated by modeling the typical 3D column collapse.

5 ACKNOWLEDGEMENTS

This work was financially supported by the National Natural Science Foundation of China (by Project Nos. 11972030 and 51909095), Research Grants Council of Hong Kong (by GRF Project No. 16207319, TBRS Project No. T22-603/15N and CRF Project No. C6012-15G)

6 REFERENCES

Guo N., Yang, Z.X., Yuan, W.H., and Zhao, J.D. 2021. A coupled SPFEM/DEM approach for multiscale modeling of largedeformation geomechanical problems. *International Journal for Numerical and Analytical Methods in Geomechanics*, 45(5), 648-667.

Christoffersen, J., Mehrabadi, M. M., & Nemat-Nasser, S. 1981. A micromechanical description of granular material behavior. *Journal* of Applied Mechanics, 48, 339.

Guo N. and Zhao J.D. 2014. A coupled FEM/DEM approach for hierarchical multiscale modelling of granular media. *International Journal for Numerical Methods in Engineering*, 99(11), 789-818.

Guo N., and Zhao, J.D. 2016. 3D multiscale modeling of strain localization in granular media. Computers and Geotechnics, 80, 360-372.

Lajeunesse E., Monnier J. B. and Homsy G. M. 2005. Granular slumping on a horizontal surface. Physics of fluids, 17(10), 103302.

Liang W.J., and Zhao J.D. 2019. Multiscale modeling of large deformation in geomechanics. *International Journal for Numerical* and Analytical Methods in Geomechanics, 43(5), 1080-1114.

Liang W.J., Zhao J.D., Wu H.R. and Soga K. 2021. Multiscale Modeling of Anchor Pullout in Sand. *Journal of Geotechnical and Geoenvironmental Engineering*, 147(9), 04021091

Nicot, F., Hadda, N., Guessasma, M., Fortin, J. and Millet, O. 2013. On the definition of the stress tensor in granular media. *International Journal of Solids and Structures*, 50, 2508–2517.

Wu H.R., Zhao J.D. and Guo, N. 2018. Multiscale insights into borehole